JMEPEG (2014) 23:2801–2808
DOI: 10.1007/s11665-014-1036-2

1059-9495/$19.00

Microstructure and Strength of Al_2O_3 and Carbon Fiber Reinforced 2024 Aluminum Alloy Composites

Jacek W. Kaczmar, Krzysztof Naplocha, and Jerzy Morgiel

(Submitted January 15, 2014; in revised form April 17, 2014; published online May 10, 2014)

The microstructure and mechanical properties of 2024 aluminum alloy composite materials strengthened with Al_2O_3 Saffil fibers or together with addition of carbon fibers were investigated. The fibers were stabilized in the preform with silica binder strengthened by further heat treatment. The preforms with 80-90% porosity were infiltrated by direct squeeze casting method. The microstructure of the as-cast specimens consisted mainly of α-dendrites with intermetallic compounds precipitated at their boundaries. The homogenization treatment of the composite materials substituted silica binder with a mixture of the Θ phase and silicon precipitates distributed in the remnants of SiO_2 amorphous phase. Outside of this area at the binder/matrix interface, fine MgO precipitates were also present. At surface of C fibers, a small amount of fine Al_3C_4 carbides were formed. During pressure infiltration of preforms containing carbon fibers under oxygen carrying atmosphere, C fibers can burn releasing gasses and causing cracks initiated by thermal stress. The examination of tensile and bending strength showed that reinforcing of aluminum matrix with 10-20% fibers improved investigated properties in the entire temperature range. The largest increase in relation to unreinforced alloy was observed for composite materials examined at the temperature of 300 °C. Substituting Al_2O_3 Saffil fibers with carbon fibers leads to better wear resistance at dry condition with no relevant effect on strength properties.

Keywords 2024 Al alloy, carbon fibers, Saffil fibers

1. Introduction

Aluminum matrix composite materials are widely applied in automotive and aviation industry, due to their high specific strength, high electrical, and thermal conductivity, as well as good wear resistance. However, the poor wettability, chemical reactions between fibers and liquid aluminum as well as fiber clustering, non-homogeneous reinforcement distribution, and porosities still restrict their wide-scale industrial application. Reinforcing of high-strength aluminum alloy with up to 20 vol.% of Al_2O_3 Saffil fibers showed increase of UTS and hardness already at ambient temperature (Ref 1, 2). Moreover, composites retain their strength by ∼100 °C higher, than the applied matrix can do. However, further optimization of properties could be achieved only by improvement of wetting during infiltration and strength of metal/ceramic interface.

The addition of elements such as Mg, Cu, Ni, and Si into the matrix alloy can improve wetting of ceramic fibers which was also proven by Sung (Ref 3). However, aside of the improved infiltration, the introduced additions caused formation of a thick layer of brittle spinel phases like $MgAl_2O_4$ or $CuAl_2O_4$ at the Saffil fiber/matrix interface (Ref 4). These negative processes could be to some extent controlled by magnesium content in the matrix, keeping the amount below 4 at.% Mg at interfaces and then only a less brittle MgO compound will form (Ref 5). The above precipitation processes are controlled by the diffusion of magnesium through vacancies of alumina and can be supported by SiO_2 binder, a less stable compound which easily releases oxygen into the matrix. Thus, any thermal loading of composite material can promote formation of brittle precipitates at ceramic/matrix interface step by step compromising its mechanical properties.

Serious problems arising in production of composite materials by pressure infiltration may also cause preform defects. The fibers can segregate or form clusters, while binder used to connect them may create so-called sails or lumps which restrain metal flow during infiltration process. Even during pressure infiltration, the local bundling of poor wetted fibers may easily trap air pockets serving next as crack nucleus resulting later in failure of the composite materials. The above presented situation is aggravated in case of the matrix of 2xxx series aluminum alloy, as they are characterized by especially poor casting properties and are rarely able to fill completely all mold cavities and fully saturate porous materials even under relatively high applied pressure. Nevertheless, only composite materials with matrix based on such high-strength aluminum alloys may compete with them in practical application.

This paper presents a thorough study of the microstructure transformation, wetting, and chemical reactions at interface during casting processes. Their effect on mechanical properties of 2024 aluminum matrix composite materials reinforced with 10-20 vol.% of Al_2O_3 fibers and in some cases also with addition of C fibers was analyzed. The fracture surface and corresponding failure mechanism were discussed and characterized by optical and electron microscopy.

Jacek W. Kaczmar and **Krzysztof Naplocha**, Institute of Production Engineering and Automation, Wroclaw University of Technology, Wroclaw, Poland; and **Jerzy Morgiel**, Institute of Metallurgy and Materials Science, Polish Academy of Sciences, Krakow, Poland. Contact e-mail: krzysztof.naplocha@ pwr.wroc.pl.

2. Experimental Procedures

The porous preforms were made of Saffi ceramic fibers and in some specimens with addition of carbon fibers provided by SGL Carbon Ltd, see Table 1. Preforms were produced through wet forming process including mixing of fibers in "water glass," i.e., $SiO_2(Na_2O)$ solution, drying, forming, and firing at 950 °C. The resulting preforms show skeleton structure of roughly randomly arranged fibers.

The infiltration of preform with 2024 aluminum alloys, see Table 2, was performed by direct squeeze casting method. The process parameters were as follows: the infiltration pressure 90 MPa, the pouring temperature of 2024 alloy 700 °C, preform temperature of 560 °C, and porosity of preform 80-90%. Composite materials and unreinforced alloy specimens were T6 heat treated and examined by applying the Instron Model 1126 strength tester at the temperature of 20, 100, 200, and 300 °C. Pin-on-disk wear tests were applied, and specimens were pressed against tool steel CT70 counterpart with forces corresponding to pressures of 0.8, 1.2, and 1.5 MPa. Microstructure and chemical transformations at the interface were analyzed by means of scanning and transmission electron microscopy Tecnai SuperTWIN FEG (200 kV) with HAADF detector.

3. Results and Discussion

3.1 Microstructure Analysis

The re-melting of delivered extruded Al2024 alloy and its subsequent squeeze casting resulted in development of cast materials microstructure with characteristic segregation of precipitates at the grain boundaries, prevailing formation of η_2-AlCu phase, $Al_{77}Cu_{17}Mn_2Fe_3$ intermetallic compounds, and α/S-Al_2CuMg eutectic mixture (Fig. 1). Generally, the precipitates in composite material are evidently refined due to the presence of large number of places available for heterogeneous nucleation. A lower volume of molten metal due to the presence of solid reinforcement released less latent heat during solidification. It causes a faster solidification of infiltrating metal inside preform leading to higher matrix saturation with copper. Therefore, even without homogenization heat treatment, the composite material may show a small positive strengthening response to aging similar to T6 treatment for its Al2024 aluminum alloy matrix.

The homogenization treatment at slightly higher parameters as compared with standard T6 conditions for Al2024 (increased temperature to 515 °C and longer time −1.5 h) enables to dissolve more Cu2Al intermetallic phases segregated at grain boundaries. Only the largest particles in the vicinity of reinforcement remain un-dissolved probably due to its stabilization with small amounts of oxygen transferred from the fibers (Fig. 2a). Outside of this area at the binder/matrix interface, MgO forms according to reaction $SiO_2 + 2\,Mg \rightarrow 2MgO + Si$ (−64 kcal/mol). In places where fibers were covered with thinner layer of binder, the latter was completely dissolved and fine MgO crystalline precipitated directly on the fiber surface (Fig. 2b). However, such prolonged heat treatment results in substituting of most of the amorphous SiO_2 bridges and connections between fibers with a mixture of dense nanocrystalline materials including the Θ′ phase and almost pure silicon (see Fig. 3).

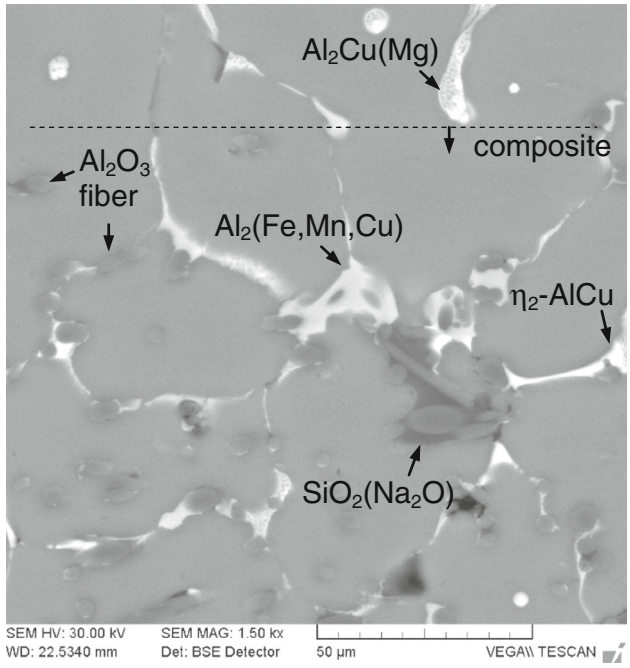

Fig. 1 Microstructure of transition zone between unreinforced as-cast 2024 alloy (top part) and reinforced with 10 vol.% Al_2O_3 fiber (bottom)

Table 1 Properties of Al_2O_3 Saffil and C fibers

Materials	Composition, wt.%	Density, g/cm^3	Tensile strength, MPa	Young modulus, GPa	Diameter, µm	Length, µm
Al_2O_3 fiber	Al_2O_3-δ: 96-97 SiO_2: 3-4	3.3	2000	300	2-4	0.1-0.3
C fiber	C: >99.9	1.8-2.0	1960	340	9-10	1-2

Table 2 Chemical composition of 2024 alloy in wt. %

Alloy	Cu	Mg	Mn	Fe	Zn	Al
2024	3.80-4.90	1.20-1.80	0.30-0.90	≤0.50	≤0.15	Balance

Furthermore, density of intermetallic phases was found higher near the matrix/fiber interfaces. Thermal mismatch of the components induces thermal-misfit dislocations at the fiber/matrix interface which can act as heterogeneous nucleation sites for precipitates. Summarizing, the amorphous SiO_2 binder was partly dissolved and acted as an oxygen source substituted partially by MgO, but the more brittle $MgAl_2O_4$ spinels were not detected. The subsequent age hardening caused the formation of the Θ platelet phase from saturated matrix at the {100} aluminum planes. It should be also noted that dissolution of amorphous silica leads to formation of microvoids, which can serve as crack nucleation sites.

To improve wear properties at dry conditions, preform was supplemented with small amount of C fibers. In such case, carbon fibers should act as lubricant pockets providing a thin carbon film separating working parts and protecting them against seizure. During infiltration of carbon fiber with aluminum matrix, they may react leading to formation of Al_4C_3. The latter could cause fast deterioration of the fiber/matrix interface and induce a high stresses within a composite. In the case of composite reinforced with fiber matting, a large gap between matrix and the fiber bundles was observed (Fig. 4a). Usually, delamination and cracking of C fiber occurred already shortly after casting or during subsequent machining of the specimens. Thermal mismatch of components caused large stresses which in the case of C fibers relates on their direction. Depending on C fiber type, the mean transverse CTE varies from 5×10^{-6} to 10×10^{-6}/K and the longitudinal one from 1.6×10^{-6} to 2.1×10^{-6}/K (Ref 6). Therefore, after cooling, fibers are under compression (CTE for the matrix is ca. 23×10^{-6}/K), with large shear forces produced at the interface. Additionally, in the case of fiber mat, separate bundles, arranged normal to each other, act alternately in tension and compression. Similar deterioration of microstructure and mechanical properties caused by the high

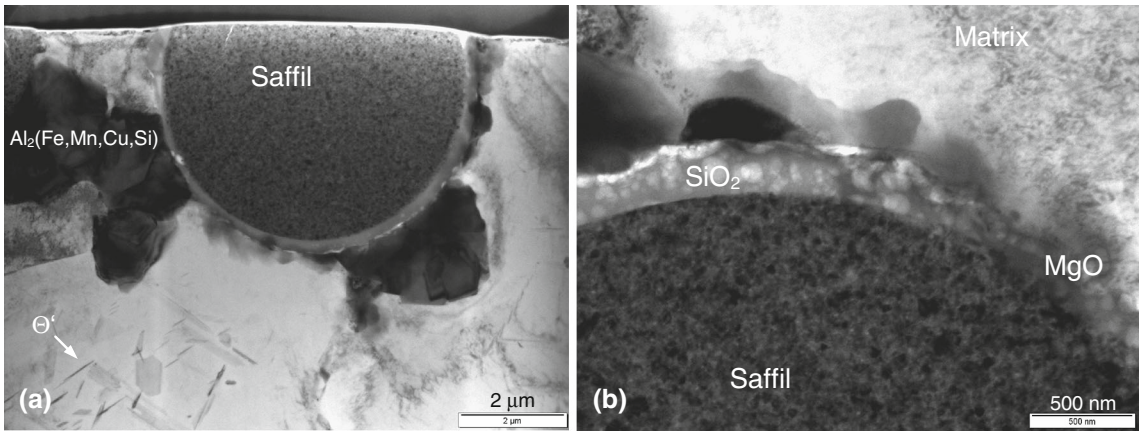

Fig. 2 Transmission electron microscopy images of Saffil fibers in 2024 matrix with intermetallic precipitates (a) and dissolution of binder layer (b)

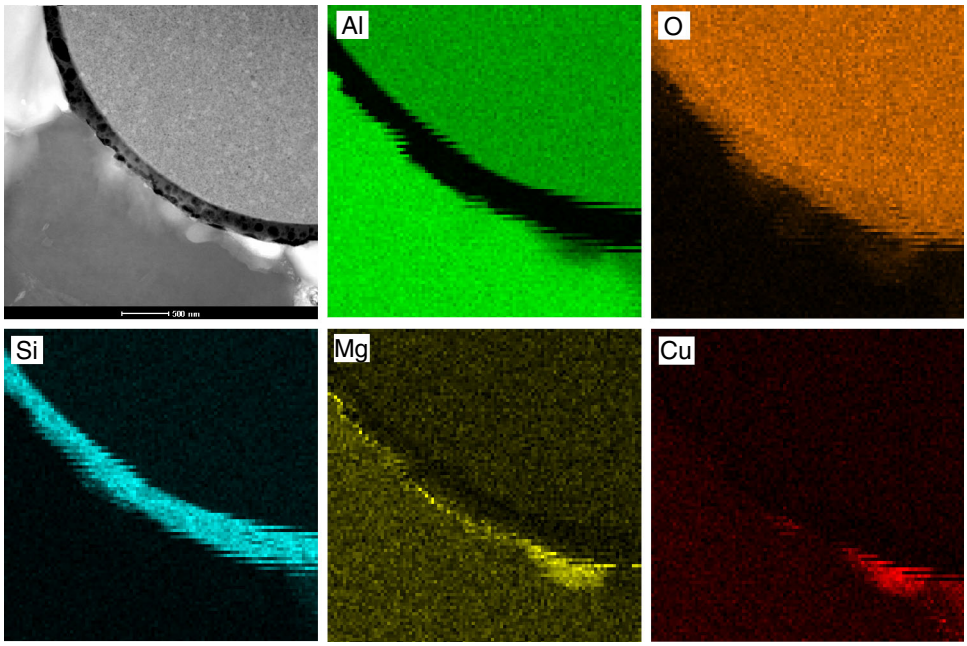

Fig. 3 Scanning-transmission (HAADF) image and maps of distribution of Al, O, Si, Mg, and Cu elements in 2024/Saffil composite

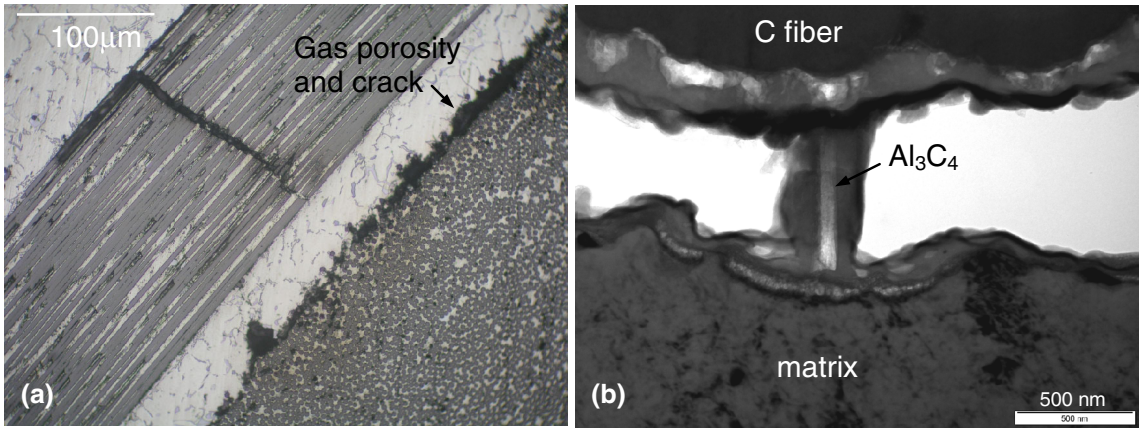

Fig. 4 Crack of C fiber bundle caused by gas porosity and thermal mismatch stresses (a), transmission images of C fibers/aluminum matrix interface with Al_3C_4 carbide (b)

residual porosity and cracks originated from shrinkage was observed in carbon fiber multilayer composites (Ref 7).

Infiltration of fiber preform requires preheating of reinforcement almost to temperature of molten metal. In squeeze casting method placed, preform in die is exposed to surrounding atmosphere. C fibers, being in contact with surrounding atmosphere, start to burn at temperature of over 560 °C. Thus, in contact with molten aluminum alloy, CO or CO_2 gases can be produced and trapped at the interface. This phenomenon was occasionally observed during carbon bundle infiltration. Usually complete solidification lasts from 15 to 20 s, so during that time, the remnants of oxygen can react and produce indicated bubbles. Near the C-fiber/aluminum matrix interface within large bubbles, a presence of Al_3C_4 carbides was occasionally noticed (Fig. 4b). It looks that at the beginning of squeeze infiltration process, molten metal came into contact with C fiber, reacted producing aluminum carbide which was next detached by newly formed gasses. It was determined (Ref 8) that in the case of carbon, wires infiltrated and exposed to the liquid aluminum already after one second carbides may be formed in rapidly increasing quantity. Fortunately, the above phenomenon was observed rather rarely. Mapping of composites reinforced additionally with carbon fiber has shown similar intermetallc distribution, though reaction of SiO_2 binder with Mg can also result in precipitation of Mg_2Si, see Fig. 5

3.2 Strength Properties

Solidification of metal under pressure increases liquidus temperature by 6-8 K/100 MPa (Ref 9), and as a result of undercooling, a finer microstructure is produced. Furthermore, during infiltration of preform at the temperature of 500-600 °C, metal quickly nucleates on fiber surfaces. Therefore, crystals inside the strengthened region are 5-10 times smaller than in the unreinforced area. Preform acts as a rigid skeleton restraining metal flow and after solidification contributes stresses due to thermal mismatch between reinforcement and Al alloy matrix. Preform coefficient of thermal expansion, being comparable with that characteristic for strengthening fibers, amounted $7\text{-}10 \times 10^{-6}$/K.

During cooling, it shrinks much less than the matrix, what causes tension stresses up to 35÷57 MPa as determined by Ref 10. During subsequent heating, the matrix expands and deforms, annihilating most of the strain. Therefore, tensile stress in the matrix and compressive stress in fibers at about 80-100 °C are fully reduced. Further heating, reverses tendency and expansion of the matrix with higher expansion coefficient ($20\text{-}24 \times 10^{-6}$/K) will be restrained by the fibers. As a result, at about 200-250 °C, local stress can achieve matrix yield point. Then the weakest areas located in the vicinity of the fibers bundle or at the fiber-matrix interface can crack even under low load during strength examinations.

Beside thermal stresses, lattice deformation with high density dislocations induces precipitation of Θ′ phase even in the as-cast matrix, what was also observed in composite materials AlCu4MgAg/SiC (Ref 5). Thus, hardness of the as-cast composite is relatively high and subsequent heat treatment only slightly enhanced its value, see Table 3. Similarly small reinforcing effect was observed in the case of Young modulus and the elongation. Alumina fibers slightly reduced the ductility of aluminum matrix presumably due to grain refinement and the strong stresses induced by the mismatch in thermal expansion between the matrix and fibers

Strength investigations performed on age hardened composite materials show slight increase of Young modulus and distinct reinforcing effect for bending and tensile strength properties. In relation to the unreinforced alloy, the bending strength of composite materials strengthened with 10% of Al_2O_3 fiber increased by ca. 100 MPa at the 20-300 °C temperature range, see Fig. 6. Higher, i.e., 20% volume content of fiber only slightly enhances this effect.

The increasing fiber volume from 10% to 20% resulted in increase of UTS up to ∼200 MPa, see Fig. 7. Strength of squeeze cast 2024 alloy was ca 230 MPa, comparable with UTS = 250 MPa obtained by Hajjari and Divandari (Ref 11). The best result was achieved at the temperature of 300 °C, at which strength of composite with 20% of fiber was ∼100% higher than that of the matrix. This corresponds to 384 MPa calculated from the rule of mixture with efficiency factor related to fiber orientation and length $\eta = 0.5$. This confirmed proper shear strength of the interface approximately equal to the matrix strength.

Observations of specimen fractures after tensile and bending examinations revealed significant amount of cracks in the matrix, adjacent to the fibers, or even propagating transversely or along fiber axes. Thus, process can be intensified by interdendritic porosities which, in strongly intertwined fiber network, are difficult to feed with liquid alloy, see Fig. 8(a).

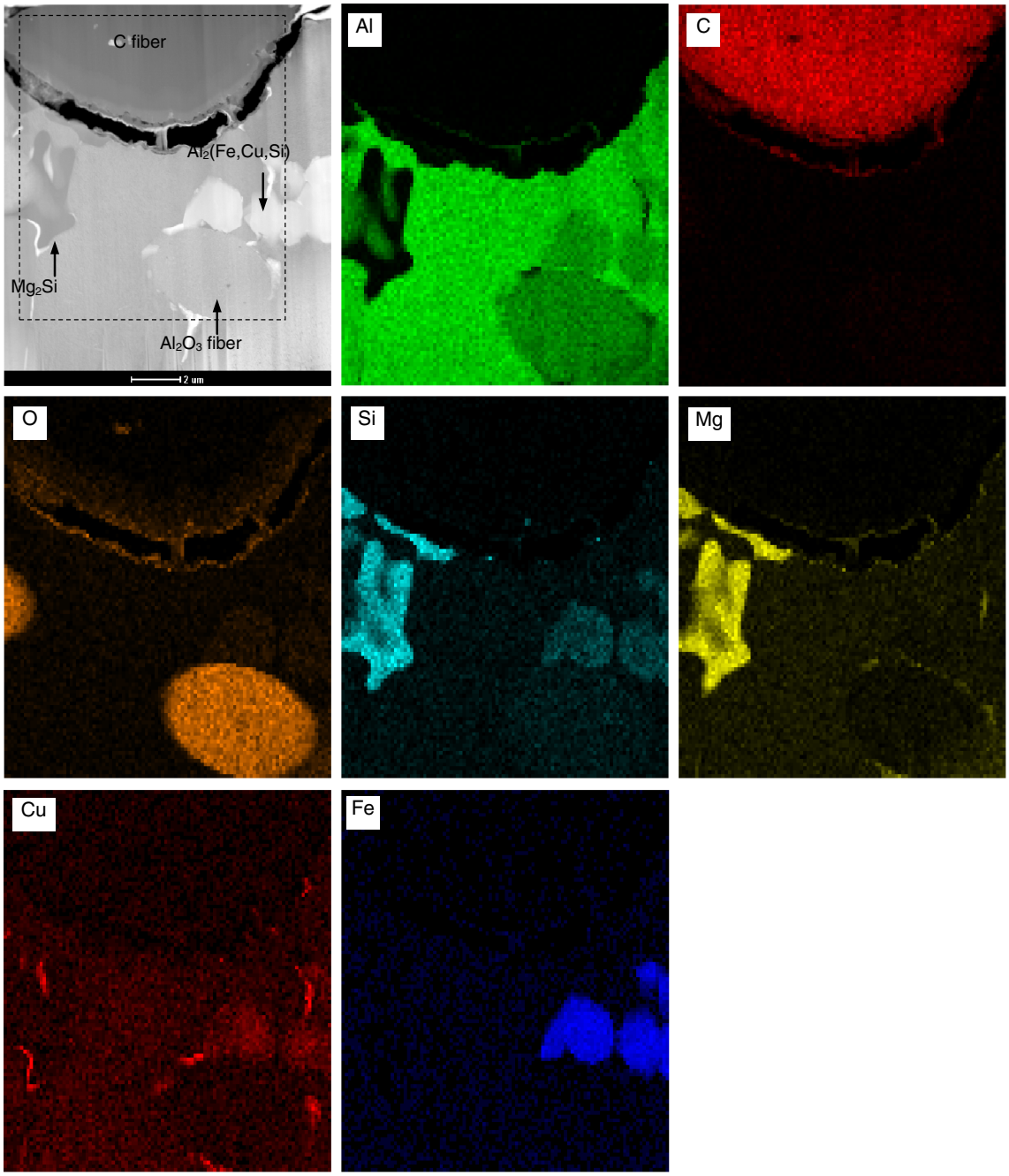

Fig. 5 Scanning-transmission (HAADF) images and mapping of Al, C, O, Si, Mg, Cu and Fe elements in 2024/Saffil/C composite materials

Table 3 Properties of the unreinforced alloy and composite materials

Material	HB as-cast	HB-T6	$E_{20\ °C}$, GPa	$E_{300\ °C}$, GPa	ε, %
2024	100 ± 4	120 ± 5	76 ± 8	45 ± 11	1.3 ± 0.6
2024 + 10% Al_2O_3 fiber	140 ± 4	160 ± 9	92 ± 6	48 ± 9	1.1 ± 0.2

Existed in Saffil fiber α-Al_2O_3 plates occurred close to microvoids, meaning that they frequently initiate crack and premature material fracture, see Fig. 8(b).

Basing on the shear-lag theory, the ratio of the maximum tensile stress in a fiber, σ_{max}, and the maximum shear stress at the end of fiber, τ_{max}, is described by equation (Ref 12):

$$\frac{\tau_{max}}{\sigma_{max}} = \sqrt{\frac{G_m}{E_f}\frac{-1}{\ln(V_f)}}, \quad \text{(Eq 1)}$$

where G_m is the matrix shear modulus, E_f is the fiber axial modulus, and V_f is the volume fraction of fibers. If the shear strength of the interface is higher, and tensile strength of fiber is smaller than the maximum stresses, then interface should withstand the local loading. However, crack may develop in the vicinity of a next fiber. On the other hand, using appropriate data for the experiment, i.e., G_m = 28 GPa, E_f = 300 GPa, V_f = 10%, the maximum shear stress at the interface can be estimated for τ_{max} = 0.201, σ_{max} = 402 MPa, what if compared with shear strength of the matrix of 283 MPa, seems unlikely. Therefore, it should be assumed that fiber cracking in semi-ordered preform is caused by accompanying bending and low matrix strength at grain boundaries.

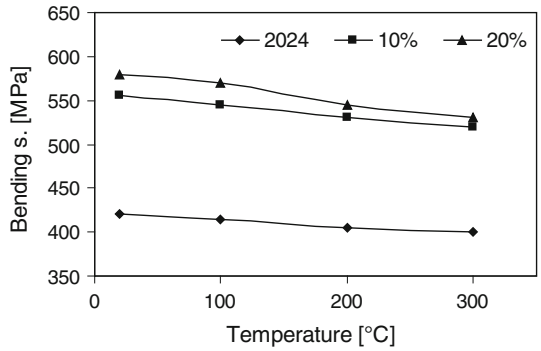

Fig. 6 Bending strength of unreinforced 2024 alloy and composite materials reinforced with 10 and 20 vol.% of Al_2O_3 fiber at the temperature range of 20-300 °C, after T6 heat treatment

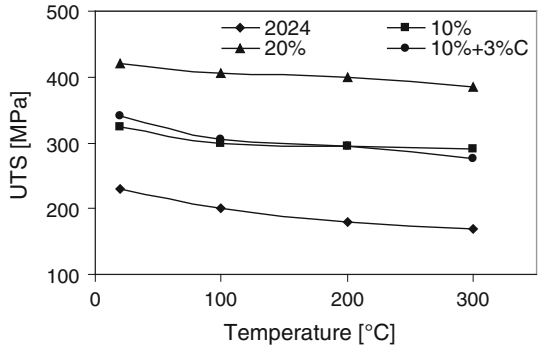

Fig. 7 UTS of unreinforced 2024 alloy and composite materials reinforced with 10 and 20 vol.% of Al_2O_3 fibers and 10 vol.% of Al_2O_3 of fibers with 3 vol.% of C fibers at the range of 20-300 °C, after T6 heat treatment

Usually strengthening fibers present at the fracture surface are strongly segmented. Even in such conditions, the ''pull-out'' effect or detaching of fiber ends, where the highest shear stresses arise, is rarely observed. Fractured fibers, from the one side, joint and anchor grains between them and on the other hand, when oriented perpendicular to direction of tension, initiate crack, and induce fracture development. Generally, in composite materials with high fiber volume fraction, the intercrystalline fracture is observed, whereas those with low reinforcement volume fraction or in matrix alloy, with larger grains, cracking in the transcrystalline way take place, see Fig. 9(b). Cracks in unreinforced volume propagate through grain boundaries whereas in the composite matrix grains are split in area with broken fibers. Reinforcement beside transferring the load and restraining stresses significantly refines microstructure. Dimension of the grains in unreinforced 2024 casting is about 50-100 μm whereas in the matrix, inside of the reinforced volume, decreases to 10-30 μm, see Fig. 9(a). Thus, this could be the predominant reinforcing effect causing increase of strength properties.

In the necking area subjected to higher load, fibers oriented parallel or at a slight angle to direction of tension were cracking at the beginning. It is because in such condition, they bear most of the acting stresses. Analyzed by Kang et al. (Ref 13), stress transfer in randomly oriented δ-Al_2O_3 fibers in composite materials confirmed that axial stresses for tilted fibers meets its minimum at 60° of orientation, whereas the highest interfacial shear stresses occurred at the angle of 45°. Thus, the most adverse fiber orientation is 60°, instead of 90°. Observations of the microstructure in the vicinity of the sample fracture, after tensile test, allowed determining the depth of cracking zone as 300-400 μm. In the vicinity of grain boundaries where lower elastic modulus and high plastic deformation occurred, fibers

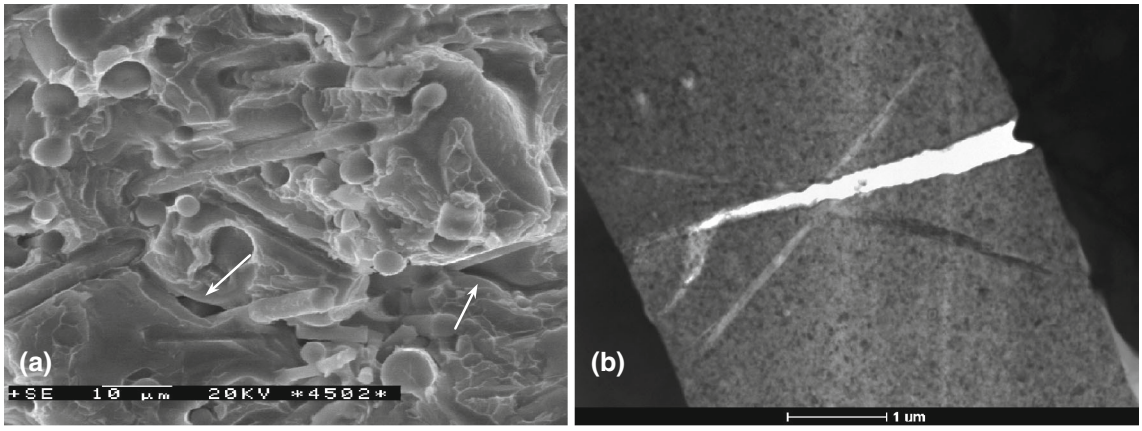

Fig. 8 Tension fracture of composite materials with interdendritic porosities (a), transmission images of crack developed in Saffil fiber with α-Al_2O_3 plates (b)

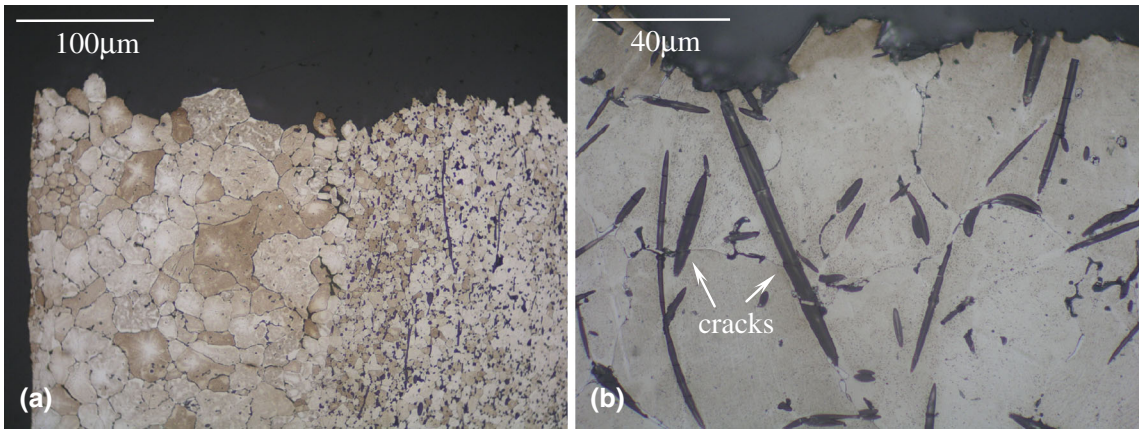

Fig. 9 Tension fracture of special specimen partly reinforced with Saffil fiber (a), cracking of fibers at grain boundaries after tension test at 100 °C (b)

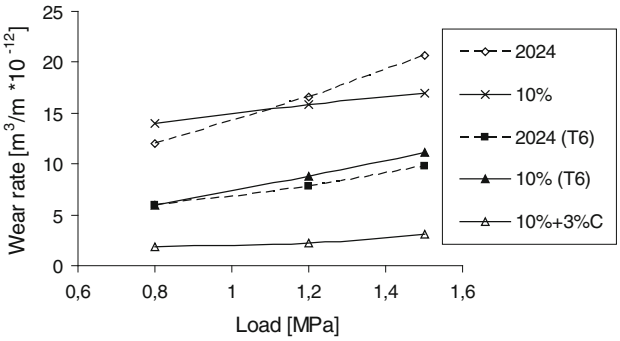

Fig. 10 Wear rate of the unreinforced 2024 alloy, as-cast, and T6 heat-treated composite materials reinforced with 10 vol.% of Saffil Al_2O_3 fibers, composite supplemented with 3 vol.% of C fibers

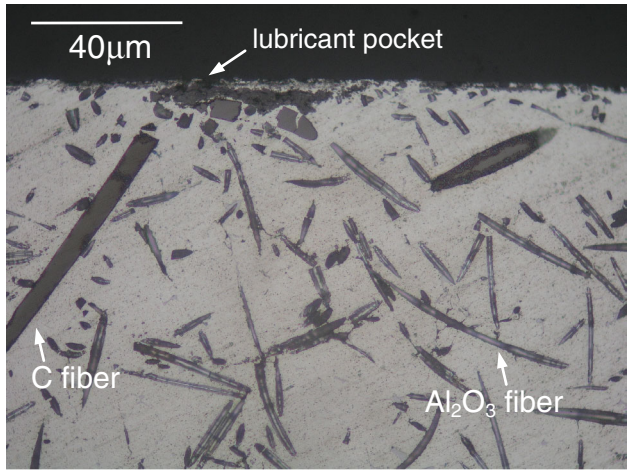

Fig. 11 Wear surface of 2024 based composite materials reinforced with 10 vol.% of Saffil Al_2O_3 fibers and 3 vol.% of carbon fibers

cracks were often observed, see Fig. 9(b). Thus, inside the grains, modulus of the matrix is higher than at the interface, and the matrix is effectively reinforced, whereas between boundaries, the most loads are transferred by strengthening fibers. According to elastic-plastic analysis (Ref 13, 14), fiber axial stresses can reach even 4000-7000 MPa, i.e., higher than their tensile strength (~2000 MPa). All these indicate that most of investigated stress transfer models considered homogeneous matrix properties, and prediction of strength properties can significantly differ from those determined experimentally.

3.3 Wear Behavior

Wear resistance of composite materials reinforced with Al_2O_3 fibers is better than matrix especially at higher load (see Fig. 10). During friction hard fragments of alumina, Saffil fibers were transferred between counterparts and composite material. Accelerated wear rate of both parts increased friction coefficient from 0.36 for unreinforced alloy to 0.45 for 2024/10% Al_2O_3 composite. Strengthening the composite material with addition of 3 vol.% of graphite fibers significantly improved wear resistance at dry condition. Usually carbon fibers, similarly as alumina fibers, restrain plastic deformation simultaneously piling up stresses and arresting dislocation (Ref 15, 16). With progress of abrasion at the wear surface, carbon fibers primarily provide lubricant film which protect against adhesion and seizure. At the wear surface, fragmented and plastically deformed matrix components can be found. Thus, graphite fibers slightly restrain deformation in subsurface, but first of all, they create solid lubricant pocket, see Fig. 11.

4. Conclusion

The microstructure, matrix-fibers interfaces, and strength properties of 2024 aluminum matrix composite materials reinforced with Saffil and carbon fibers were described. Strength properties significantly depend on interfacial bonding formed during manufacturing and T6 heat treatment. However, the pressure infiltration of Saffil fibers with 2024 aluminum alloy can induce chemical reaction leading to formation of brittle phase at fiber/matrix interface. The conclusions are listed as follows:

1. Heat treatment applied for the homogenization of the composite matrix causes partial dissolution of SiO_2 binder and its substitution with nanocrystalline material containing the Θ′ phase. At the binder/aluminum matrix interface, MgO was formed. Incorporating carbon fibers

by squeeze casting method can induce formation of Al_3C_4 at the interface.
2. During tensile or bending tests, pull-out of fibers was rarely observed. Under fracture surface, broken fibers zone reached a depth of 200-300 μm. Unreinforced alloy cracked with intercrystalline fracture, whereas composites by transcrystalline way.
3. Reinforcing of aluminum alloys with 10-20% of Al_2O_3 Saffil fibers enhanced tensile and bending strength in 20-300 °C temperature range. The T6 heat-treated composite materials reinforced 20% of fibers exhibited highest improvement of strength.
4. Only addition of carbon fiber can essentially reduce wear rate by creating carbon containing solid lubricant film.

Acknowledgment

This work was supported by the EU FP7 Project "Micro and Nanocrystalline Functionally Graded Materials for Transport Applications" (MATRANS) under Grant Agreement No. "228869."

Open Access

References

1. C. Badini, P. Fino, M. Musso, and P. Dinardo, Thermal Fatigue Behaviour of a 2014/Al_2O_3-SiO_2 (Saffil® Fibers) Composite Processed by Squeeze Casting, *Mater. Chem. Phys.*, 2000, **64**(3), p 247–255
2. N. Sobczak, J. Sobczak, R. Asthana, and R. Purgert, The Mystery of Molten Metal, *Chine Foundry*, 2010, **7**, p 425–437
3. Y.-M. Sung, Calcia-Alumina Fibre-Reinforced Al 7075 Alloy Composites Produced by Melt-Infiltration: Interfacial Wetting and Reaction, *J. Mater. Sci.*, 1997, **32**, p 1069–1073
4. S. Wang and H.J. Dudek, Fiber-Matrix Interaction in the α-Al_2O_3 Fiber Reinforced Aluminium Piston Alloy, *Mater. Sci. Eng.*, 1996, **A205**, p 180–186
5. S. Long, O. Beffort, C. Cayron, and C. Bonjour, Microstructure and Mechanical Properties of a High Volume Fraction SiC Particle Reinforced $AlCu_4MgAg$ Squeeze Casting, *Mater. Sci. Eng. A*, 1999, **269**(1-2), p 175–185
6. C. Pradere and C. Sauder, Transverse and Longitudinal Coefficient of Thermal Expansion of Carbon Fibers at High Temperatures (300-2500 K), *Carbon*, 2008, **46**(14), p 1874–1884
7. L. Fuso, D. Manfredi, S. Biamino, M. Pavese, P. Fino, and C. Badini, SiC-Based Multilayered Composites Containing Short Carbon Fibres Obtained by Tape Casting, *Compos. Sci. Technol.*, 2009, **69**(11-12), p 1772–1776
8. J.T. Blucher, J. Dobranszky, and U. Narusawa, Aluminium Double Composite Structures Reinforced with Composite Wires, *Mater. Sci. Eng. A*, 2004, **387-389**, p 867–872
9. T.M. Yue and G.A. Chadwick, Squeeze Casting of Light Alloys and Their Composites, *J. Mater. Process. Technol.*, 1996, **58**, p 302–307
10. Y.D. Huang, N. Hort, and K.U. Kainer, Thermal Behavior of Short Fiber Reinforced AlSi12CuMgNi Piston Alloy, *Composites*, 2004, **A35**, p 249–263
11. E. Hajjari and M. Divandari, An Investigation on the Microstructure and Tensile Properties of Direct Squeeze Cast and Gravity Die Cast 2024 Wrought Al Alloy, *Mater. Des.*, 2008, **29**, p 1685–1689
12. S. Fukumoto, A. Hirose, and K.F. Kobayashi, Evaluation of the Strength of Diffusion Bonded Joints in Continuous Fiber Reinforced Metal Matrix Composites, *J. Mater. Process. Technol.*, 1997, **68**, p 184–191
13. G.-Z. Kang, C. Yang, and J. Zhang, Tensile Properties of Randomly Oriented Short δ-Al_2O_3 Fiber Reinforced Aluminum Alloy Composites. I. Microstructure Characteristics, Fracture Mechanisms and Strength Prediction, *Composites A Appl. Sci. Manuf.*, 2002, **33**(5), p 647–656
14. T. Okabe, M. Nishikawa, N. Takeda, and H. Sekine, Effect of Matrix Hardening on the Tensile Strength of Alumina Fiber-Reinforced Aluminum Matrix Composites, *Acta Mater.*, 2006, **54**(9), p 2557–2566
15. A. Daoud, Wear Performance of 2014 Al Alloy Reinforced with Continuous Carbon Fibers Manufactured by Gas Pressure Infiltration, *Mater. Lett.*, 2004, **58**(25), p 3206–3213
16. J. Du, Y. Liu, S. Yu, and W. Li, Dry Sliding Friction and Wear Properties of Al_2O_3 and Carbon Short Fibres Reinforced Al-12Si Alloy Hybrid Composites, *Wear*, 2004, **257**(9-10), p 930–940